Available online at www.sciencedirect.com
ScienceDirect
Journal of Sound and Vibration 317 (2008) 537–556
JOURNAL OF SOUND AND VIBRATION
www.elsevier.com/locate/jsvi

Parameter-dependent input-delayed control of uncertain vehicle suspensions

Haiping Du[a,*], Nong Zhang[a], James Lam[b]

[a]*Mechatronics and Intelligent Systems, Faculty of Engineering, University of Technology, Sydney, P.O. Box 123, Broadway, NSW 2007, Australia*
[b]*Department of Mechanical Engineering, The University of Hong Kong, Pokfulam Road, Hong Kong*

Received 11 October 2007; received in revised form 18 February 2008; accepted 29 March 2008
Handling Editor: L.G. Tham
Available online 4 June 2008

Abstract

This paper presents a parameter-dependent controller design approach for vehicle active suspensions to deal with changes in vehicle inertial properties and existence of actuator time delays. By defining a parameter-dependent Lyapunov functional, matrix inequality conditions with reduced conservatism are obtained for the design of controllers. Feasible solutions can be obtained by solving a finite number of linear matrix inequalities (LMIs) embedded within a genetic algorithm (GA). Both state feedback and static output feedback controllers can be designed under a unified framework. Based on the measurement or estimation of the vehicle inertial parameters, a parameter-dependent controller could be implemented in practice. The presented approach is applied to a two-degree-of-freedom quarter-car suspension model. Numerical simulations on both bump and random road responses show that the designed parameter-dependent controllers can achieve good active suspension performance regardless of the variation on the sprung mass and the presence of actuator time delay.

1. Introduction

Vehicle active suspensions have been studied for many years and different methods have been proposed to improve vehicle suspension performances [1,2]. Ride comfort, handling or road holding capability, and suspension deflection limitation, are often considered by automotive makers as the most important performance issues in the design of an advanced vehicle suspension system. These performances, however, are conflicting in the sense that they involve tradeoff amongst each other. Consequently, multiobjective control of vehicle suspensions [3–7] has attracted much attention recently because it can reduce the conservatism of the approach that minimises different performance requirements with one single weighted objective.

Changes in vehicle inertial properties, such as vehicle sprung mass, vehicle centre of gravity, and vehicle pitch, roll, and yaw moments of inertia about the vehicle centre of gravity, are mostly occurred in sport utility

*Corresponding author.
E-mail addresses: haipingdu68@yahoo.co.uk, Haiping_Du@hotmail.com (H. Du).

0022-460X/$ - see front matter © 2008 Elsevier Ltd. All rights reserved.
doi:10.1016/j.jsv.2008.03.066

vehicles (SUVs), military and commercial vehicles, and small and light vehicles in which ratio of passenger/cargo to the vehicle unsprung mass can have a large variation. It has been widely documented that changes in vehicle inertial properties have direct effects on vehicle ride comfort, handling, and braking performances. Therefore, to achieve more stringent levels of comfort, safety, and fuel efficiency, an accurate estimation of the vehicle inertial properties becomes necessary. Currently, both on-line and off-line estimation methods have been developed to identify the vehicle inertial parameters based on easily obtained information [8–11]. With the development of accurate estimation on vehicle inertial parameters, parameter-dependent control technique could be applied to realise robust control of vehicle suspensions regardless of changes in vehicle inertial parameters.

Practical considerations of the realisation of active suspensions in real-world applications include choosing appropriate actuators that can fit into the suspension packaging space and satisfy the practical power and bandwidth requirements, as well as choosing available measurements for feedback control. Compared to the electromagnetic actuators, electrohydraulic actuators have been considered as one of the most viable choices for an active suspension due to their high power-to-weight ratio and low cost. Nevertheless, as explained in Ref. [12], using electrohydraulic actuators to track the desired forces is fundamentally limited in its ability when interacting with an environment possessing dynamics. In particular, time delays obviously exist in these actuators when tracking a desired force [12,13]. Neglecting these time delays may affect the control performance and even render the control system unstable [14,15]. To overcome the actuator time-delay problem, one method is to design a controller using the integrated system model in which the actuator's dynamics are included [16–19]. The other method is to include the actuator time delay into the controller design process [15,20] and to design a controller that can robustly stabilise the system and can guarantee the system performance in spite of the existence of time delay. On the issue of choosing available measurements for feedback control of vehicle suspension, static output feedback control strategy would be the best choice because it can use the easily measurable variables, such as suspension deflection and suspension travel velocity, as feedback signals to realise the active vehicle suspensions [21].

Although load-dependent controllers were developed in Ref. [7] to deal with the vehicle sprung mass variation problem, the actuator time-delay problem is not considered in that work. On the contrary, in the work of Du and Zhang [15], the actuator time-delay problem was addressed, without considering the vehicle inertial parameter uncertainties. In this paper, the parameter-dependent control strategy is applied to design the robust vehicle active suspensions that consider both the vehicle inertial parameter variations and the actuator time delays. By defining the parameter-dependent Lyapunov functional [22–25], matrix inequalities with reduced conservatism for designing such kinds of controllers are derived. The feasible solutions can be obtained by solving a finite number of linear matrix inequalities (LMIs) embedded within a genetic algorithm (GA). Both state feedback and static output feedback controllers can be designed using the same methodology. Finally, the presented approach is applied to a two-degree-of-freedom quarter-car suspension model. Numerical simulations on both bump and random road responses show that the designed parameter-dependent controller can achieve good active suspension performances in spite of the variation of vehicle sprung mass and the presence of actuator time delay.

The subsequent parts of this paper are organised as follows. Section 2 presents the problem formulation for the robust control of vehicle active suspensions. The design approach for the parameter-dependent controller based on the solvability of LMIs is presented in Section 3. Section 4 presents the design results and performance evaluation. Finally, we conclude our findings in Section 5.

Notation: $\mathbb{R}^n$ denotes the n-dimensional Euclidean space, and $\mathbb{R}^{n\times m}$ is the set of all $n \times m$ real matrices. For a real symmetric matrix W, the notation $W>0$ ($W<0$) is used to denote its positive- (negative-) definiteness. Also, I is used to denote the identity matrix of appropriate dimensions. To simplify notation, $*$ is used to represent a block matrix which is readily inferred by symmetry.

2. Problem formulation

In this study, a two-degree-of-freedom quarter-car suspension model shown in Fig. 1 is considered for controller design. This model has been used extensively in the literature because it can capture many important characteristics of many complicated suspension models. For the quarter-car suspension model shown in Fig. 1,

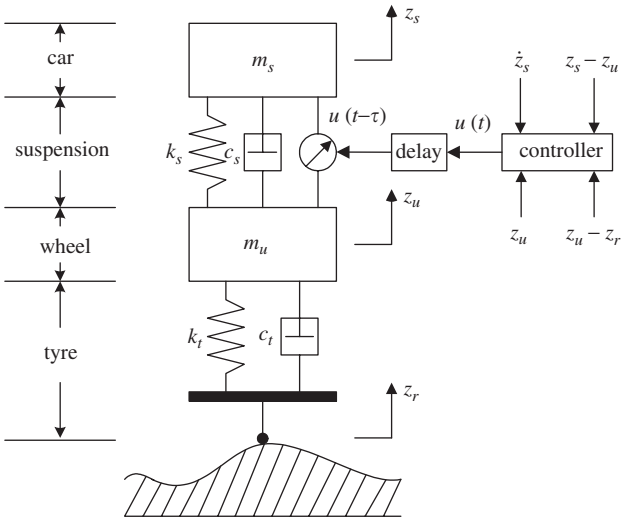

Fig. 1. Quarter-car active suspension model.

the governing equations of motion for the sprung and unsprung masses can be expressed as

$$m_s\ddot{z}_s(t) + c_s[\dot{z}_s(t) - \dot{z}_u(t)] + k_s[z_s(t) - z_u(t)] = u(t),$$

$$m_u\ddot{z}_u(t) + c_s[\dot{z}_u(t) - \dot{z}_s(t)] + k_s[z_u(t) - z_s(t)] + k_t[z_u(t) - z_r(t)] + c_t[\dot{z}_u(t) - \dot{z}_r(t)] = -u(t), \tag{1}$$

where m_s is the sprung mass, which represents the car chassis; m_u is the unsprung mass, which represents the wheel assembly; c_s and k_s are damping and stiffness of the passive suspension, respectively; k_t and c_t stand for compressibility and damping of the pneumatic tyre, respectively; $z_s(t)$ and $z_u(t)$ are the displacements of the sprung and unsprung masses, respectively; $z_r(t)$ is the road displacement input; $u(t)$ represents the active control force, which is generally provided by means of hydraulic actuator placed between sprung mass and unsprung mass of vehicle suspension.

By defining the state variable as

$$x(t) = [x_1(t)\ \ x_2(t)\ \ x_3(t)\ \ x_4(t)]^{\mathrm{T}}, \tag{2}$$

where

$$x_1(t) = z_s(t) - z_u(t),\ \text{suspension deflection},$$

$$x_2(t) = z_u(t) - z_r(t),\ \text{tyre deflection},$$

$$x_3(t) = \dot{z}_s(t),\ \text{sprung mass velocity},$$

$$x_4(t) = \dot{z}_u(t),\ \text{unsprung mass velocity},$$

Eq. (1) is written in state-space form as

$$\dot{x}(t) = Ax(t) + B_1w(t) + B_2u(t), \tag{3}$$

where $x(t) \in \mathbb{R}^4$, $w(t) \in \mathbb{R}$, $u(t) \in \mathbb{R}$, $A \in \mathbb{R}^{4\times4}$, $B_1 \in \mathbb{R}^{4\times1}$, $B_2 \in \mathbb{R}^{4\times1}$, and

$$A = \begin{bmatrix} 0 & 0 & 1 & -1 \\ 0 & 0 & 0 & 1 \\ -k_s/m_s & 0 & -c_s/m_s & c_s/m_s \\ k_s/m_u & -k_t/m_u & c_s/m_u & -(c_s+c_t)/m_u \end{bmatrix},$$

$$B_1 = [0\ \ -1\ \ 0\ \ c_t/m_u]^{\mathrm{T}},$$

$$B_2 = [0 \;\; 0 \;\; 1/m_s \;\; -1/m_u]^{\mathrm{T}}, \quad w(t) = \dot{z}_r(t).$$

In this paper, the three performance aspects for a quarter-car suspension system are taken into account.

2.1. Ride comfort

Ride comfort can be quantified by the sprung mass acceleration, therefore, the sprung mass acceleration is chosen as the first control output, i.e.,

$$z_1(t) = \ddot{z}_s(t), \tag{4}$$

where $\ddot{z}_s(t)$ can be derived from Eq. (3). In order to design an active suspension to perform adequately in a wide range of shock and vibration environments, the H_∞ norm is chosen as the performance measure since H_∞ norm of a linear time-invariant (LTI) system is equal to the energy-to-energy gain and its value actually gives an upper bound on the root-mean-square (rms) gain. Hence, our goal is to minimise the H_∞ norm of the transfer function $T_{z_1 w}$ from the disturbance $w(t)$ to the control output $z_1(t)$ to improve the ride comfort performance.

2.2. Suspension deflection limitation

In order to avoid damaging vehicle components and generating more passenger discomfort, the active suspension controller must be capable of preventing the suspension from hitting its travel limit. Therefore, we need to guarantee the suspension deflection

$$|z_s(t) - z_u(t)| \leqslant z_{\max}, \tag{5}$$

where $z_{\max}$ is the maximum suspension deflection hard limit, under any road disturbance input and vehicle running conditions. The suspension travel space does not need to be minimal but its peak value needs to be constrained. Since an H_∞ norm of a mathematical function in time-domain actually defines the peak value of the function, i.e.,

$$\|z\|_\infty \triangleq \sup_{t\in[0,\infty)} \sqrt{z^{\mathrm{T}}(t)z(t)}, \tag{6}$$

it is able to optimise the H_∞ norm of the suspension deflection output under the energy-bounded road disturbance input, that is,

$$\|w\|_2 \triangleq \sqrt{\int_0^\infty w^{\mathrm{T}}(t)w(t)\,\mathrm{d}t} < \infty, \tag{7}$$

i.e., $w \in L_2[0,\infty)$, to realise the hard requirement for the suspension deflection. This is generalised H_2 (GH_2) or energy-to-peak optimisation problem [26].

2.3. Road holding ability

In order to ensure a firm uninterrupted contact of wheels to road, the dynamic tyre load should not exceed the static one [27], i.e.,

$$k_t(z_u(t) - z_r(t)) < 9.8(m_s + m_u). \tag{8}$$

This is also a peak value optimisation problem which can be dealt with the same way as the suspension deflection. Hence, we define the hard constraints on the suspension deflection and the tyre load as the second control output, i.e.,

$$z_2(t) = \begin{bmatrix} (z_s(t) - z_u(t))/z_{\max} \\ k_t(z_u(t) - z_r(t))/9.8(m_s + m_u) \end{bmatrix}. \tag{9}$$

In summary, the vehicle suspension control system is described as

$$\begin{aligned} \dot{x}(t) &= Ax(t) + B_1 w(t) + B_2 u(t), \\ z_1(t) &= C_1 x(t) + D_{12} u(t), \\ z_2(t) &= C_2 x(t), \\ y(t) &= Cx(t), \end{aligned} \tag{10}$$

where $y(t) \in \mathbb{R}^n$ is the measurement output, n ($1 \leqslant n \leqslant 4$) is the number of measurement variables, $C_1 \in \mathbb{R}^{1\times 4}$, $C_2 \in \mathbb{R}^{2\times 4}$, $D_{12} \in \mathbb{R}^1$, and

$$C_1 = [-k_s/m_s \;\; 0 \;\; -c_s/m_s \;\; c_s/m_s], \quad D_{12} = 1/m_s, \quad C_2 = \begin{bmatrix} 1/z_{\max} & 0 & 0 & 0 \\ 0 & k_t/9.8(m_s+m_u) & 0 & 0 \end{bmatrix}.$$

Matrix $C \in \mathbb{R}^{n\times 4}$ is defined in terms of the available measurements. For state feedback controller design, $C = I$.

When changes in vehicle inertial properties and actuator time delays are considered in Eq. (10), the vehicle model becomes an uncertain model with input delay and this model can be expressed as a parameter-dependent model given by

$$\begin{aligned} \dot{x}(t) &= A(\alpha)x(t) + B_1(\alpha)w(t) + B_2(\alpha)u(t-\tau), \\ z_1(t) &= C_1(\alpha)x(t) + D_{12}(\alpha)u(t-\tau), \\ z_2(t) &= C_2(\alpha)x(t), \\ y(t) &= Cx(t), \\ x(t) &= \phi(t), \quad \forall t \in [-\tau, 0], \end{aligned} \tag{11}$$

where τ is the actuator time delay satisfying $0 < \tau \leqslant \bar{\tau}$, where $\bar{\tau}$ is the delay bound, $\phi(t)$ is the initial condition. Matrices $A(\alpha)$, $B_1(\alpha)$, $B_2(\alpha)$, $C_1(\alpha)$, $C_2(\alpha)$, and $D_{12}(\alpha)$ are functions of α which is the uncertain parameter vector.

Assume matrices $A(\alpha)$, $B_1(\alpha)$, $B_2(\alpha)$, $C_1(\alpha)$, $C_2(\alpha)$, and $D_{12}(\alpha)$ are constrained within the polytope $\mathscr{P}$ given by

$$\mathscr{P} = \left\{ \begin{array}{c} (A, B_1, B_2, C_1, C_2, D_{12})(\alpha): \\ (A, B_1, B_2, C_1, C_2, D_{12})(\alpha) = \sum_{i=1}^{N} \alpha_i (A, B_1, B_2, C_1, C_2, D_{12})_i, \\ \sum_{i=1}^{N} \alpha_i = 1, \;\; \alpha_i \geqslant 0, \;\; i = 1, \ldots, N. \end{array} \right\}, \tag{12}$$

It is clear from Eq. (12) that the knowledge of the value of α_i defines a precisely known system (11) inside the polytope $\mathscr{P}$ described by the convex combination of its N vertices. Throughout the paper, the vertices of the polytope $\mathscr{P}$ are denoted as $A_i, B_{1i}, B_{2i}, C_{1i}, C_{2i}, D_{12i}$, $i = 1, \ldots, N$. In practice, based on the developed identification method [11], the inertial parameters could be measured or estimated on-line so that the value of α_i can be found.

In this paper, the aim of the robust active suspension design is to find a parameter-dependent control law

$$u(t) = K(\alpha)y(t) = K(\alpha)Cx(t) = \left(\sum_{i=1}^{N} \alpha_i K_i\right) Cx(t), \;\; \sum_{i=1}^{N} \alpha_i = 1, \;\; \alpha_i \geqslant 0, \;\; i = 1, \ldots, N, \tag{13}$$

where $K_i \in \mathbb{R}^{1\times n}$ is the control gain matrix to be designed, such that the closed-loop system given by

$$\begin{aligned} \dot{x}(t) &= A(\alpha)x(t) + B_1(\alpha)w(t) + B_2(\alpha)K(\alpha)Cx(t-\tau), \\ z_1(t) &= C_1(\alpha)x(t) + D_{12}(\alpha)K(\alpha)Cx(t-\tau), \\ z_2(t) &= C_2(\alpha)x(t), \\ x(t) &= \phi(t), \quad \forall t \in [-\tau, 0], \end{aligned} \tag{14}$$

has the following properties: (i) the closed-loop system (14) is asymptotically stable; (ii) the performance $\|T_{z_1w}\|_\infty < \gamma_1$ is minimised subject to $\|z_2\|_\infty < \gamma_2\|w\|_2$ for all non-zero $w \in L_2[0,\infty)$ and the prescribed constant $\gamma_2 > 0$, where T_{z_1w} denotes the closed-loop transfer function from the road disturbance $w(t)$ to the control output $z_1(t)$.

3. Parameter-dependent controller design

The sufficient conditions for the robust asymptotically stable of closed-loop system (14) and performance requirements can be derived as follows.

Define a parameter-dependent Lyapunov–Krasovskii functional candidate as

$$V(t,\alpha) \triangleq x^{\mathrm{T}}(t)P(\alpha)x(t) + \int_{-\tau}^{0}\int_{t+s}^{t} \dot{x}^{\mathrm{T}}(\theta)Q(\alpha)\dot{x}(\theta)\,\mathrm{d}\theta\,\mathrm{d}s, \tag{15}$$

where

$$P(\alpha) = \sum_{i=1}^{N}\alpha_i P_i,\ \ Q(\alpha) = \sum_{i=1}^{N}\alpha_i Q_i \tag{16}$$

and $P_i \in \mathbb{R}^{4\times4}$, $P_i = P_i^{\mathrm{T}} > 0$, $Q_i \in \mathbb{R}^{4\times4}$, $Q_i = Q_i^{\mathrm{T}} > 0$ are matrices to be determined. Then, the derivative of $V(t,\alpha)$ along the solution of system (14) is given by

$$\begin{aligned}\dot{V}(t,\alpha) &= \dot{x}^{\mathrm{T}}(t)P(\alpha)x(t) + x^{\mathrm{T}}(t)P(\alpha)\dot{x}(t) + \tau\dot{x}^{\mathrm{T}}(t)Q(\alpha)\dot{x}(t) - \int_{t-\tau}^{t}\dot{x}(\theta)Q(\alpha)\dot{x}(\theta)\,\mathrm{d}\theta\\ &\leqslant \dot{x}^{\mathrm{T}}(t)P(\alpha)x(t) + x^{\mathrm{T}}(t)P(\alpha)\dot{x}(t) + \bar{\tau}\dot{x}^{\mathrm{T}}(t)Q(\alpha)\dot{x}(t) - \int_{t-\tau}^{t}\dot{x}(\theta)Q(\alpha)\dot{x}(\theta)\,\mathrm{d}\theta\\ &= \frac{1}{\tau}\int_{t-\tau}^{t}\Phi(t,\theta)\,\mathrm{d}\theta,\end{aligned} \tag{17}$$

where $\Phi(t,\theta) = \dot{x}^{\mathrm{T}}(t)P(\alpha)x(t) + x^{\mathrm{T}}(t)P(\alpha)\dot{x}(t) + \bar{\tau}\dot{x}^{\mathrm{T}}(t)Q(\alpha)\dot{x}(t) - \tau\dot{x}(\theta)Q(\alpha)\dot{x}(\theta)$. By the Newton–Leibniz formula, we have

$$x(t) - x(t-\tau) = \int_{t-\tau}^{t}\dot{x}(\theta)\,\mathrm{d}\theta. \tag{18}$$

Then, for any matrices

$$R(\alpha) = \sum_{i=1}^{N}\alpha_i R_i,\ \ S(\alpha) = \sum_{i=1}^{N}\alpha_i S_i,\ \ T(\alpha) = \sum_{i=1}^{N}\alpha_i T_i, \tag{19}$$

where $R_i \in \mathbb{R}^{4\times4}$, $S_i \in \mathbb{R}^{4\times4}$, and $T_i \in \mathbb{R}^{4\times4}$, we have

$$\frac{2}{\tau}\int_{t-\tau}^{t}[x^{\mathrm{T}}(t)R(\alpha) + x^{\mathrm{T}}(t-\tau)S(\alpha) + \dot{x}^{\mathrm{T}}(t)T(\alpha)][x(t) - x(t-\tau) - \tau\dot{x}(\theta)]\,\mathrm{d}\theta = 0. \tag{20}$$

Moreover, according to Eq. (14), for any matrices $U \in \mathbb{R}^{4\times4}$, $V \in \mathbb{R}^{4\times4}$, and $W \in \mathbb{R}^{4\times4}$, we have

$$\frac{2}{\tau}\int_{t-\tau}^{t}[x^{\mathrm{T}}(t)U + x^{\mathrm{T}}(t-\tau)V + \dot{x}^{\mathrm{T}}(t)W][\dot{x}(t) - A(\alpha)x(t) - B_1(\alpha)w(t) - B_2(\alpha)K(\alpha)Cx(t-\tau)]\,\mathrm{d}\theta = 0. \tag{21}$$

Adding Eqs. (20) and (21) to Eq. (17) yields

$$\dot{V}(t,\alpha) \leqslant \frac{1}{\tau}\int_{t-\tau}^{t}\eta^{\mathrm{T}}(t,\theta)\Pi(\alpha)\eta(t,\theta)\,\mathrm{d}\theta, \tag{22}$$

where $\eta^{\mathrm{T}}(t,\theta)=[x^{\mathrm{T}}(t)\ \ x^{\mathrm{T}}(t-\tau)\ \ \dot{x}^{\mathrm{T}}(t)\ \ \dot{x}^{\mathrm{T}}(\theta)\ \ w^{\mathrm{T}}(t)]$ and

$$\Pi(\alpha)=\begin{bmatrix}\Pi_{11} & \Pi_{12} & \Pi_{13} & -\tau R(\alpha) & -UB_1(\alpha)\\ * & \Pi_{22} & \Pi_{23} & -\tau S(\alpha) & -VB_1(\alpha)\\ * & * & \Pi_{33} & -\tau T(\alpha) & -WB_1(\alpha)\\ * & * & * & -\tau Q(\alpha) & 0\\ * & * & * & * & 0\end{bmatrix}, \tag{23}$$

where

$$\begin{aligned}
\Pi_{11} &= R(\alpha)+R(\alpha)^{\mathrm{T}}-UA(\alpha)-A^{\mathrm{T}}(\alpha)U^{\mathrm{T}},\\
\Pi_{12} &= -R(\alpha)+S^{\mathrm{T}}(\alpha)-UB_2(\alpha)K(\alpha)C-A^{\mathrm{T}}(\alpha)V^{\mathrm{T}},\\
\Pi_{13} &= P(\alpha)+U+T^{\mathrm{T}}(\alpha)-A^{\mathrm{T}}(\alpha)W^{\mathrm{T}},\\
\Pi_{22} &= -S(\alpha)-S^{\mathrm{T}}(\alpha)-VB_2(\alpha)K(\alpha)C-C^{\mathrm{T}}K^{\mathrm{T}}(\alpha)B_2^{\mathrm{T}}(\alpha)V^{\mathrm{T}},\\
\Pi_{23} &= V-T^{\mathrm{T}}(\alpha)-C^{\mathrm{T}}K^{\mathrm{T}}(\alpha)B_2^{\mathrm{T}}(\alpha)W^{\mathrm{T}},\\
\Pi_{33} &= \bar{\tau}Q(\alpha)+W+W^{\mathrm{T}}
\end{aligned} \tag{24}$$

and the asterisk symbol (∗) represents a term that is induced by symmetry. For example, the last row of Eq. (23) is induced as $[-B_1^{\mathrm{T}}(\alpha)U^{\mathrm{T}}\ \ -B_1^{\mathrm{T}}(\alpha)V^{\mathrm{T}}\ \ -B_1^{\mathrm{T}}(\alpha)W^{\mathrm{T}}\ \ 0\ \ 0]$. It is noted from Eq. (22) that if $\Pi(\alpha)<0$, we have $\dot{V}(t,\alpha)<0$, then system (14) with $w(t)=0$, parameter uncertainty (12), and time delay τ satisfying $0<\tau\leqslant\bar{\tau}$ is robust asymptotically stable for all uncertain parameter α.

Next, we will establish the H_∞ performance of the uncertain delay system under zero initial condition, that is, $\phi(t)=0,\quad \forall t\in[-\tau,0]$, and $V(t,\alpha)|_{t=0}=0$. Consider the following index:

$$J_1\triangleq\int_0^\infty[z_1^{\mathrm{T}}(t)z_1(t)-\gamma_1^2w^{\mathrm{T}}(t)w(t)]\,\mathrm{d}t, \tag{25}$$

then, for any non-zero $w\in L_2[0,\infty)$, there holds,

$$\begin{aligned}
J_1 &\leqslant \int_0^\infty[z_1^{\mathrm{T}}(t)z_1(t)-\gamma_1^2w^{\mathrm{T}}(t)w(t)]\,\mathrm{d}t+V(t,\alpha)|_{t=\infty}-V(t,\alpha)|_{t=0}\\
&= \int_0^\infty[z_1^{\mathrm{T}}(t)z_1(t)-\gamma_1^2w^{\mathrm{T}}(t)w(t)+\dot{V}(t,\alpha)]\,\mathrm{d}t.
\end{aligned} \tag{26}$$

After some algebraic manipulations, we obtain

$$z_1^{\mathrm{T}}(t)z_1(t)-\gamma_1^2w^{\mathrm{T}}(t)w(t)+\dot{V}(t,\alpha)\leqslant\frac{1}{\tau}\int_{t-\tau}^{t}\eta^{\mathrm{T}}(t,\theta)\bar{\Pi}(\alpha)\eta(t,\theta)\,\mathrm{d}\theta, \tag{27}$$

where

$$\bar{\Pi}(\alpha)=\begin{bmatrix}\Pi_{11}+C_1^{\mathrm{T}}(\alpha)C_1(\alpha) & \Pi_{12}+C_1^{\mathrm{T}}(\alpha)D_{12}(\alpha)K(\alpha)C & \Pi_{13} & -\tau R(\alpha) & -UB_1(\alpha)\\ * & \Pi_{22}+(D_{12}(\alpha)K(\alpha)C)^{\mathrm{T}}(D_{12}(\alpha)K(\alpha)C) & \Pi_{23} & -\tau S(\alpha) & -VB_1(\alpha)\\ * & * & \Pi_{33} & -\tau T(\alpha) & -WB_1(\alpha)\\ * & * & * & -\tau Q(\alpha) & 0\\ * & * & * & * & -\gamma_1^2\end{bmatrix}. \tag{28}$$

Then, if $\bar{\Pi}(\alpha)<0$, we have $z_1^{\mathrm{T}}(t)z_1(t)-\gamma_1^2 w^{\mathrm{T}}(t)w(t)+\dot{V}(t,\alpha)<0$, therefore $J_1<0$, and hence $\|z_1\|_2<\gamma_1\|w\|_2$ is satisfied for any non-zero $w\in L_2[0,\infty)$. Applying the Schur complement, $\bar{\Pi}(\alpha)<0$ is equivalent to

$$\hat{\Pi}(\alpha)=\begin{bmatrix} \Pi_{11} & \Pi_{12} & \Pi_{13} & -R(\alpha) & -UB_1(\alpha) & C_1^{\mathrm{T}}(\alpha) \\ * & \Pi_{22} & \Pi_{23} & -S(\alpha) & -VB_1(\alpha) & (D_{12}(\alpha)K(\alpha)C)^{\mathrm{T}} \\ * & * & \Pi_{33} & -T(\alpha) & -WB_1(\alpha) & 0 \\ * & * & * & -\bar{\tau}^{-1}Q(\alpha) & 0 & 0 \\ * & * & * & * & -\gamma_1^2 & 0 \\ * & * & * & * & * & -I \end{bmatrix}<0. \tag{29}$$

Now substitute $P(\alpha)$, $Q(\alpha)$ defined in Eq. (16) and $R(\alpha)$, $S(\alpha)$, $T(\alpha)$ defined in Eq. (19) into $\hat{\Pi}(\alpha)$, we obtain

$$\hat{\Pi}(\alpha)=\sum_{i=1}^{N}\alpha_i^2\hat{\Pi}_{ii}+\sum_{i=1}^{N-1}\sum_{j=i+1}^{N}\alpha_i\alpha_j\hat{\Pi}_{ij}, \tag{30}$$

where

$$\hat{\Pi}_{ii}=\begin{bmatrix} \Pi_{11_{ii}} & \Pi_{12_{ii}} & \Pi_{13_{ii}} & -R_i & -UB_{1_i} & C_{1_i}^{\mathrm{T}} \\ * & \Pi_{22_{ii}} & \Pi_{23_{ii}} & -S_i & -VB_{1_i} & (D_{12_i}K_iC)^{\mathrm{T}} \\ * & * & \Pi_{33_{ii}} & -T_i & -WB_{1_i} & 0 \\ * & * & * & -\bar{\tau}^{-1}Q_i & 0 & 0 \\ * & * & * & * & -\gamma_1^2 & 0 \\ * & * & * & * & * & -I \end{bmatrix}, \tag{31}$$

$$\begin{aligned} \Pi_{11_{ii}} &= R_i+R_i^{\mathrm{T}}-UA_i-A_i^{\mathrm{T}}U^{\mathrm{T}}, \\ \Pi_{12_{ii}} &= -R_i+S_i^{\mathrm{T}}-UB_{2_i}K_iC-A_i^{\mathrm{T}}V^{\mathrm{T}}, \\ \Pi_{13_{ii}} &= P_i+U+T_i^{\mathrm{T}}-A_i^{\mathrm{T}}W^{\mathrm{T}}, \\ \Pi_{22_{ii}} &= -S_i-S_i^{\mathrm{T}}-VB_{2_i}K_iC-(B_{2_i}K_iC)^{\mathrm{T}}V^{\mathrm{T}}, \\ \Pi_{23_{ii}} &= V-T_i^{\mathrm{T}}-(B_{2_i}K_iC)^{\mathrm{T}}W^{\mathrm{T}}, \\ \Pi_{33_{ii}} &= \bar{\tau}Q_i+W+W^{\mathrm{T}} \end{aligned} \tag{32}$$

and

$$\hat{\Pi}_{ij}=\begin{bmatrix} \Pi_{11_{ij}} & \Pi_{12_{ij}} & \Pi_{13_{ij}} & -(R_i+R_j) & -U(B_{1_i}+B_{1_j}) & (C_{1_i}+C_{1_j})^{\mathrm{T}} \\ * & \Pi_{22_{ij}} & \Pi_{23_{ij}} & -(S_i+S_j) & -V(B_{1_i}+B_{1_j}) & (D_{12_i}K_jC+D_{12_j}K_iC)^{\mathrm{T}} \\ * & * & \Pi_{33_{ij}} & -(T_i+T_j) & -W(B_{1_i}+B_{1_j}) & 0 \\ * & * & * & -\bar{\tau}^{-1}(Q_i+Q_j) & 0 & 0 \\ * & * & * & * & -2\gamma_1^2 & 0 \\ * & * & * & * & * & -2I \end{bmatrix}, \tag{33}$$

where

$$\begin{aligned} \Pi_{11_{ij}} &= (R_i+R_j)+(R_i+R_j)^{\mathrm{T}}-U(A_i+A_j)-(A_i+A_j)^{\mathrm{T}}U^{\mathrm{T}}, \\ \Pi_{12_{ij}} &= -(R_i+R_j)+(S_i+S_j)^{\mathrm{T}}-U(B_{2_i}K_jC+B_{2_j}K_iC)-(A_i+A_j)^{\mathrm{T}}V^{\mathrm{T}}, \\ \Pi_{13_{ij}} &= (P_i+P_j)+2U+(T_i+T_j)^{\mathrm{T}}-(A_i+A_j)^{\mathrm{T}}W^{\mathrm{T}}, \end{aligned}$$

$$\begin{aligned}
\Pi_{22_{ij}} &= -(S_i+S_j)-(S_i+S_j)^{\mathrm{T}}-V(B_{2_i}K_jC+B_{2_j}K_iC)-(B_{2_i}K_jC+B_{2_j}K_iC)^{\mathrm{T}}V^{\mathrm{T}},\\
\Pi_{23_{ij}} &= 2V-(T_i+T_j)^{\mathrm{T}}-(B_{2_i}K_jC+B_{2_j}K_iC)^{\mathrm{T}}W^{\mathrm{T}},\\
\Pi_{33_{ij}} &= \bar{\tau}(Q_i+Q_j)+2W+2W^{\mathrm{T}}.
\end{aligned} \tag{34}$$

Therefore, to ensure $\hat{\Pi}(\alpha)<0$, it is equivalent to simultaneously guaranteeing

$$\hat{\Pi}_{ii}<0, \tag{35}$$

for $i=1,\ldots,N$, and

$$\hat{\Pi}_{ij}<0, \tag{36}$$

for $i=1,\ldots,N-1$, and $j=i+1,\ldots,N$.

Furthermore, using Schur complement, the feasibility of the following inequality:

$$\begin{bmatrix} P(\alpha) & C_2^{\mathrm{T}}(\alpha) \\ C_2(\alpha) & \gamma_2^2/\gamma_1^2 \end{bmatrix}>0 \tag{37}$$

guarantees $C_2^{\mathrm{T}}(\alpha)C_2(\alpha)<\gamma_2^2/\gamma_1^2P(\alpha)$. At the same time, it can be derived from Eqs. (15) and (25) that $x^{\mathrm{T}}(t)P(\alpha)x(t)<\gamma_1^2\int_0^t w^{\mathrm{T}}(s)w(s)\,\mathrm{d}s$ if $\hat{\Pi}(\alpha)<0$ is guaranteed. Then, it can be easily established from Eqs. (14) and (37) that for all $t\geqslant 0$,

$$z_2^{\mathrm{T}}(t)z_2(t)=x^{\mathrm{T}}(t)C_2^{\mathrm{T}}(\alpha)C_2(\alpha)x(t)<\gamma_2^2/\gamma_1^2x^{\mathrm{T}}(t)P(\alpha)x(t)<\gamma_2^2\int_0^t w^{\mathrm{T}}(s)w(s)\,\mathrm{d}s\leqslant\gamma_2^2\int_0^\infty w^{\mathrm{T}}(s)w(s)\,\mathrm{d}s. \tag{38}$$

Taking the supremum over $t\geqslant 0$ yields $\|z\|_\infty<\gamma_2\|w\|_2$ for all $w\in L_2[0,\infty)$, that is, the GH_2 performance is established.

Similarly, to guarantee Eq. (37), it is equivalent to ensuring

$$\begin{bmatrix} P_i & C_{2_i}^{\mathrm{T}} \\ C_{2_i} & \gamma_2^2/\gamma_1^2 \end{bmatrix}>0, \tag{39}$$

for $i=1,\ldots,N$, and

$$\begin{bmatrix} P_i+P_j & (C_{2_i}+C_{2_j})^{\mathrm{T}} \\ C_{2_i}+C_{2_j} & 2\gamma_2^2/\gamma_1^2 \end{bmatrix}>0, \tag{40}$$

for $i=1,\ldots,N-1$, and $j=i+1,\ldots,N$.

In summary, if there exist matrices $P_i>0$, $Q_i>0$, R_i, S_i, T_i, K_i, $i=1,\ldots,N$, matrices U, V, W and scalars $\gamma_1>0$, $\gamma_2>0$ such that matrix inequalities (35), (36), (39), and (40) are satisfied simultaneously, then, closed-loop system (14) is asymptotically stable with the performance $\|T_{z_1w}\|_\infty<\gamma_1$ and $\|z_2\|_\infty<\gamma_2\|w\|_2$.

When K_i is unknown, matrix inequalities (35) and (36) are non-convex, and cannot be resolved using convex optimisation algorithm. However, for the state feedback control case, i.e., $C=I$, two possible approaches may be used to design the controller. One possible method is to try to use some matrix inequalities to transform the non-convex optimisation problem to the convex optimisation problem [28]. Another possible method is to use the cone complementarity linearisation (CCL) method to solve the controller design problem as that done in Ref. [29]. Nevertheless, for the present non-convex optimisation problem, finding an appropriate matrix bounding inequality and designing a static output feedback controller are not straightforward using the two methods mentioned earlier. On the other hand, to this kind of problem, GA is found to be very effective [30]. Hence, in this paper, when we assume $\bar{\tau}$ is given, we will use GA to solve the problem of

$$\min_{K_i}\ \gamma_1 \quad \text{subject to LMIs (35), (36), (39), and (40),} \tag{41}$$

where K_i is initially randomly generated by GA and then evolved in terms of the objective presented in Eq. (41). For a known K_i, matrix inequalities (35), (36), (39), and (40) are LMIs and can be efficiently resolved

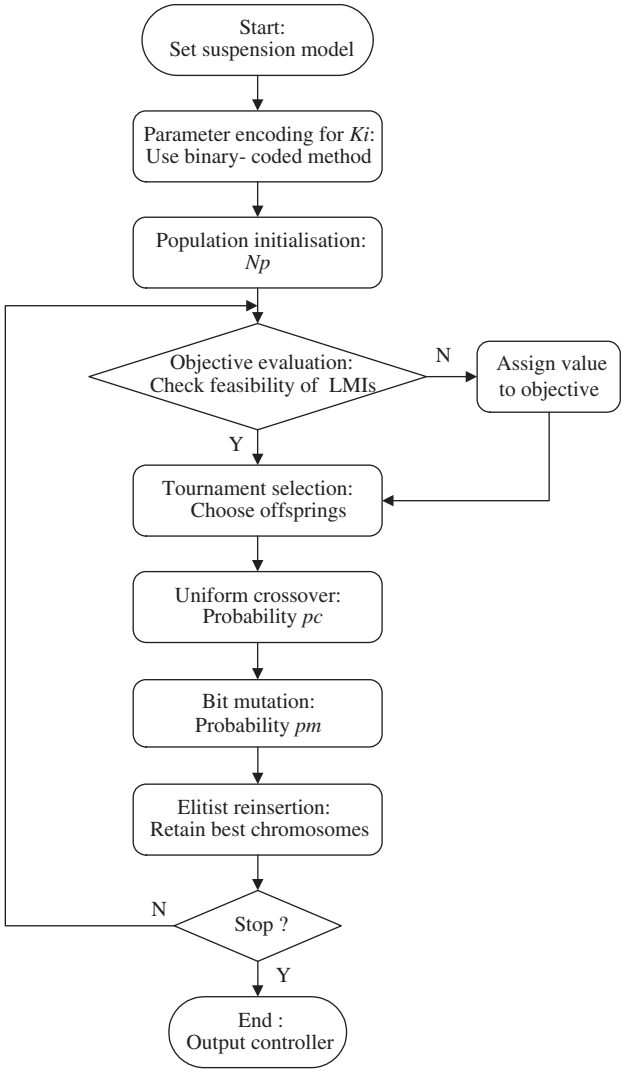

Fig. 2. Flow diagram of the proposed GA/LMI algorithm.

using Matlab LMI Toolbox. The flow diagram of the proposed GA/LMI algorithm for problem (41) is outlined in Fig. 2.

In Fig. 2, parameter encoding is used to convert the feedback gain matrix $K_i, i = 1, \ldots, N$, into a row vector with binary-coded method. Population initialisation is used to randomly generate an initial population of N_p chromosomes for K_i within a given search space. Much attention is paid to the objective evaluation step. In this step, the initial population produced in previous step is decoded into real value for every controller gain matrix K_{ij}, $j = 1, 2, \ldots, N_p$. If problem (41) with K_{ij} is feasible, then determine the minimal γ_{1j} by solving LMIs (35), (36), (39), and (40), and take every γ_{1j} as the objective value corresponding to K_{ij} and associate every K_{ij} with a suitable fitness value according to rank-based fitness assignment approach, and then go to next step. If problem (41) with K_{ij} is infeasible, the objective value corresponding to K_{ij} will be assigned a large value in order to reduce its opportunity to be survived in the next generation. Since for a feasibility problem defined by LMI constraint of the form $L(x) < R(x)$, where x is a feasible value of the vector of decision variables, a feasible solution can be found by using the auxiliary convex program, i.e., minimise β subject to $L(x) < R(x) + \beta I$, the solution to the LMI $L(x) < R(x)$ is feasible if and only if the global minimum of β is negative, and the value of β can indicate the closeness of the decision variable to the solution. Therefore, a

large value will be associated to the value of β so that more potential K_{ij} can be evolved to find the solution. Tournament selection, uniform crossover, bit mutation, and elitist reinsertion are standard evolutionary operators, which can be found in most references about GA. When the evolution process repeats for N_g generations, the algorithm stops, and the best chromosome is decoded into realvalues to produce again the control gain matrix K_i. At last, the obtained parameter-dependent control gain is given as $K(\alpha) = \sum_{i=1}^{N} \alpha_i K_i$, $\sum_{i=1}^{N} \alpha_i = 1$, $\alpha_i \geqslant 0$, $i = 1, \ldots, N$.

It is noted that GA is an evolutionary algorithm with built-in randomness. It cannot guarantee to find the optimal results every time. Hence, running the same algorithm for many times to find the possible optimal results is often necessary. In addition, if the presented GA/LMI algorithm cannot obtain a solution to a given problem after running several times, some parameters used in the algorithm, such as the population size, the controller parameter search space, the time delay bound, and the uncertain parameter variation range, should be modified. However, there is no guarantee that a suitable solution can be located if the feasible solution set is small.

4. Application to quarter-car suspension control

Now, we will apply the proposed approach to design the parameter-dependent controller for a quarter-car suspension model shown in Fig. 1. The parameters of the quarter-car suspension model selected for this study are listed in Table 1 and the maximum suspension deflection is defined as $z_{\max} = 0.08\,\text{m}$.

In this example, only vehicle sprung mass m_s is assumed to be varying due to vehicle load variation and m_s can fluctuate around its nominal value by 20%. The relationship between the uncertain parameter vector $\alpha \triangleq [\alpha_1, \alpha_2]$ and the estimation of sprung mass m_s is given as

$$\alpha_1 = \frac{1/m_s - 1/m_{s\max}}{1/m_{s\min} - 1/m_{s\max}},\ \alpha_2 = \frac{1/m_{s\min} - 1/m_s}{1/m_{s\min} - 1/m_{s\max}}, \tag{42}$$

where $m_{s\max}$ and $m_{s\min}$ denote the maximum and the minimum sprung mass allowable, respectively. It can be seen from Eq. (42) that $\alpha_1 + \alpha_2 = 1$ and $\alpha_1 \geqslant 0$, $\alpha_2 \geqslant 0$. Using the above-defined vector α, the parameter-dependent model shown in Eq. (12) can be defined. The actuator time delay bound $\bar{\tau} = 50\,\text{ms}$ is assumed. The basic GA parameters used in this paper are given as the population size $N_p = 80$; the probability of crossover $p_c = 0.8$; the probability of mutation $p_m = 0.02$; and the maximum generation $N_g = 300$. The controller parameter search space is defined as $[-10^4 \ \ 10^4]$ and the algorithm is independently run 50 times for each case.

In order to validate the designed vehicle suspension performance in time domain, examinations of the response quantities will be done to evaluate the suspension characteristics taking into account the shock and vibration [1] road profiles. In this section, two kinds of controller design problems will be studied.

4.1. Full state feedback control case

In this case, we assume that all the state variables defined in Eq. (2) for a quarter-car suspension model are measurements available, we can design a full state feedback parameter-dependent controller by solving the problem (41). The obtained controller gains are given as

$$K_1 = 10^3 \times [-2.8529 \ \ 2.8372 \ \ -2.6676 \ \ -0.0435],\ K_2 = 10^3 \times [-2.9608 \ \ 2.8117 \ \ -2.4160 \ \ -0.0469].$$

The performance of active suspension with the designed controller is evaluated via following simulations.

Table 1
Parameter values used in a quarter-car suspension model

Parameter	m_s	k_s	c_s	k_t	c_t	m_u
Value	320 kg	18 kN/m	1 kN s/m	200 kN/m	0	40 kg

Firstly, an isolated bump in an otherwise smooth road surface is used. The corresponding ground displacement for the wheel is given by

$$z_r(t) = \begin{cases} \frac{a}{2}\left(1 - \cos\left(\frac{2\pi v_0}{l}t\right)\right), & 0 \leqslant t \leqslant \frac{l}{v_0}, \\ 0, & t > \frac{l}{v_0}, \end{cases} \tag{43}$$

where a and l are the height and the length of the bump. We choose $a = 0.1\,\text{m}$, $l = 10\,\text{m}$, and the vehicle forward velocity as $v_0 = 45\,\text{km/h}$.

When actuator time delay is zero, i.e., $\tau = 0\,\text{ms}$, the bump responses of the passive suspension and the active suspension are compared in Fig. 3, where bump responses of the sprung mass acceleration, suspension deflection, tyre deflection, and active force are plotted. For clarity, only the nominal case where the sprung mass is used as its nominal value, 320 kg, and the two-vertex cases where the sprung mass is used as its maximum value, 384 kg, and its minimum value, 256 kg, respectively, are plotted. It can be seen from Fig. 3 that all the responses of the sprung mass acceleration for active suspension are lower than those of the passive suspension no matter what value the sprung mass is. Compared to the passive suspension, the suspension deflection and the tyre deflection of active suspension are all guaranteed to be less than their hard limits as

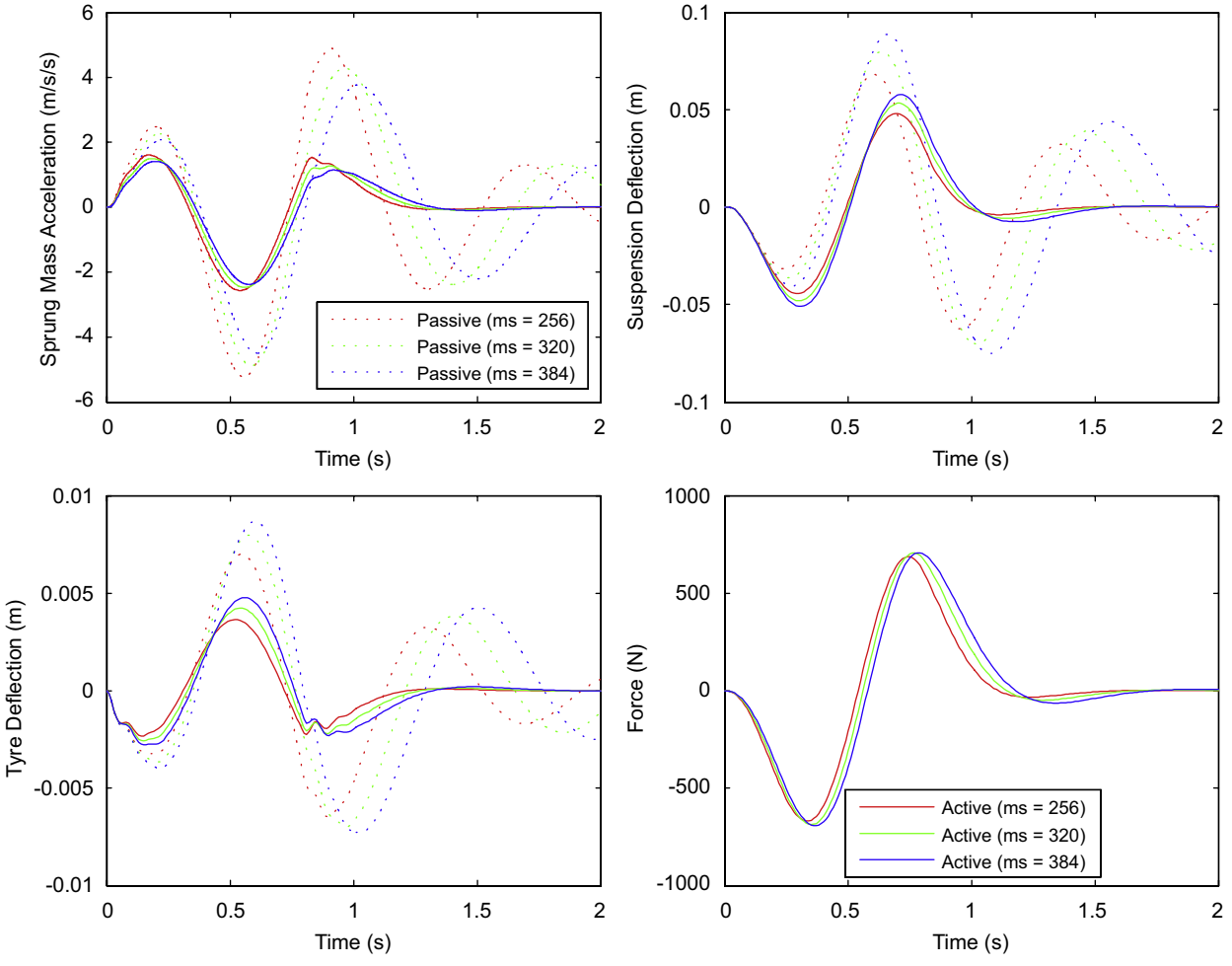

Fig. 3. Bump response for full state feedback control case with time delay $\tau = 0\,\text{ms}$. The legends shown in upper-left and lower-right plots are used for all plots in this figure.

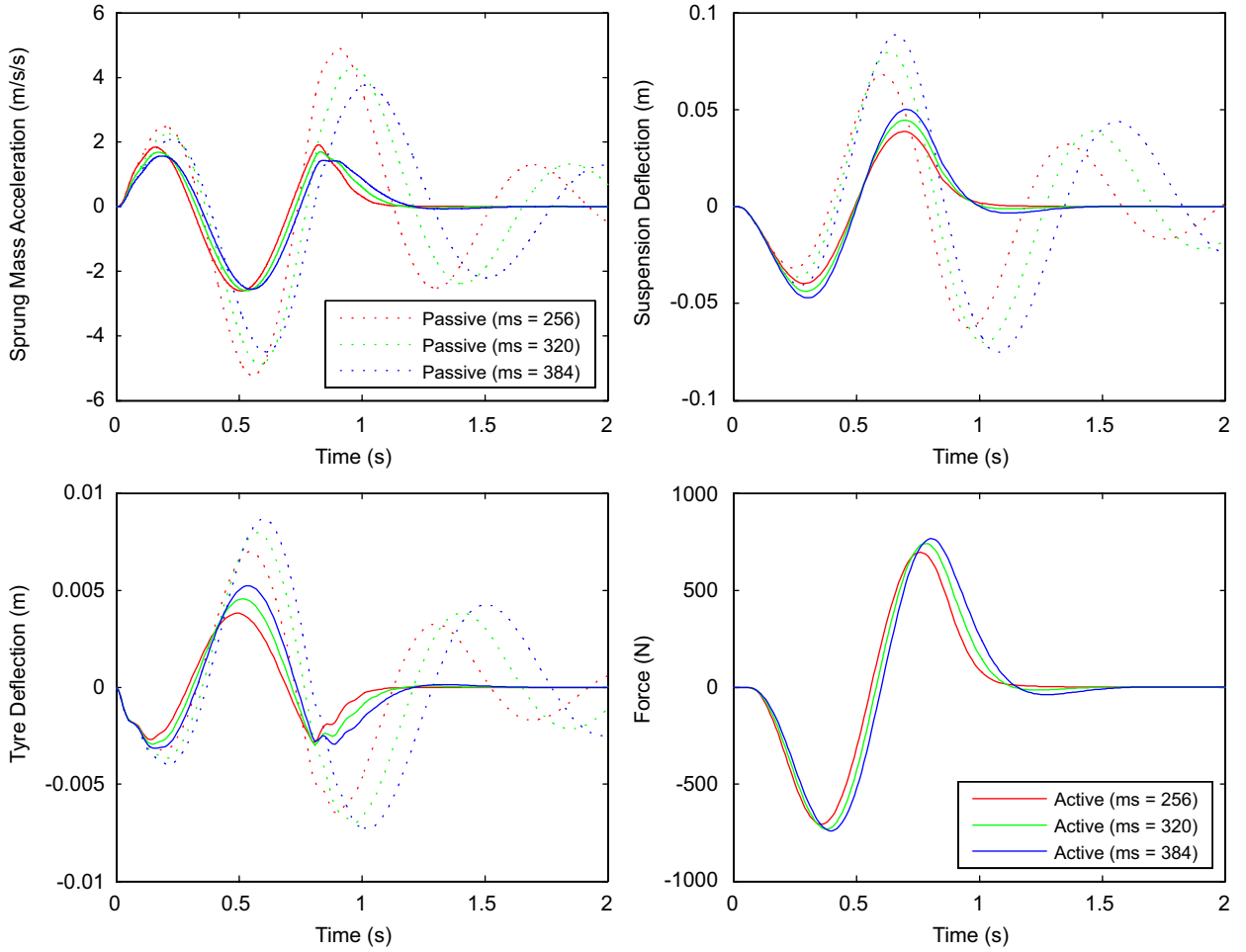

Fig. 4. Bump response for full state feedback control case with time delay $\tau = 50$ ms. The legends shown in upper-left and lower-right plots are used for all plots in this figure.

Table 2
Comparison of maximum peak value for bump response (full state feedback control case)

	Passive			Active					
				$\tau = 0$ ms			$\tau = 50$ ms		
m_s (kg)	256	320	384	256	320	384	256	320	384
$\ddot{x}_{3\max}$ (m/s^2)	5.2255	4.8756	4.4959	2.5649	2.4700	2.3771	2.6043	2.5978	2.5570
$x_{1\max}$ (m)	0.0681	0.0799	0.0889	0.0481	0.0533	0.0578	0.0396	0.0446	0.0502
$x_{2\max}$ (m)	0.0070	0.0080	0.0087	0.0036	0.0042	0.0048	0.0038	0.0046	0.0052
$u_{\max}$ (N)	–	–	–	687.05	706.18	708.42	705.94	742.23	766.46

those defined in Eqs. (5) and (8) in spite of the large bump energy. In addition, the active force is within a reasonable range which can be generated by a hydraulic actuator in practice. It is confirmed that the designed robust active suspension can realise the good suspension performance when driving over a pronounced bump road regardless of the sprung mass variation.

When actuator time delay is 50 ms, the bump responses of the passive suspension and the active suspension are compared in Fig. 4, where bump responses of the sprung mass acceleration, suspension deflection, tyre

deflection, and active force are plotted for the nominal and the two-vertex cases. It can be seen from Fig. 4 that the responses of the sprung mass acceleration, the suspension deflection, the tyre deflection, and the active force of active suspension are all similar to those shown in Fig. 3 in spite of the presence of time delay. It is validated that the designed robust active suspension can achieve good suspension performance regardless of the sprung mass variation and the actuator time delay within given bounds.

To clearly show the results, the maximum peak values of the bump responses for sprung mass acceleration, suspension deflection, tyre deflection, and active force are listed in Table 2. From Table 2, it can be seen that even when the actuator time delay presents, the maximum peak values realised by active suspension are similar to those without time-delay cases.

Secondly, when the road disturbance is considered as random vibration, it is consistent and typically specified as random process with a ground displacement power spectral density (PSD) of

$$S_g(\Omega) = \begin{cases} S_g(\Omega_0)\left(\dfrac{\Omega}{\Omega_0}\right)^{-n_1}, & \text{if } \Omega \leqslant \Omega_0, \\ S_g(\Omega_0)\left(\dfrac{\Omega}{\Omega_0}\right)^{-n_2}, & \text{if } \Omega > \Omega_0, \end{cases} \tag{44}$$

Table 3
Road roughness values classified by ISO

Degree of roughness $S_g(\Omega_0)$ (10^{-6} m^3)			
Road class	B (Good)	C (Average)	D (Poor)
Range	8–32	32–128	128–512
Geometric mean	16	64	256

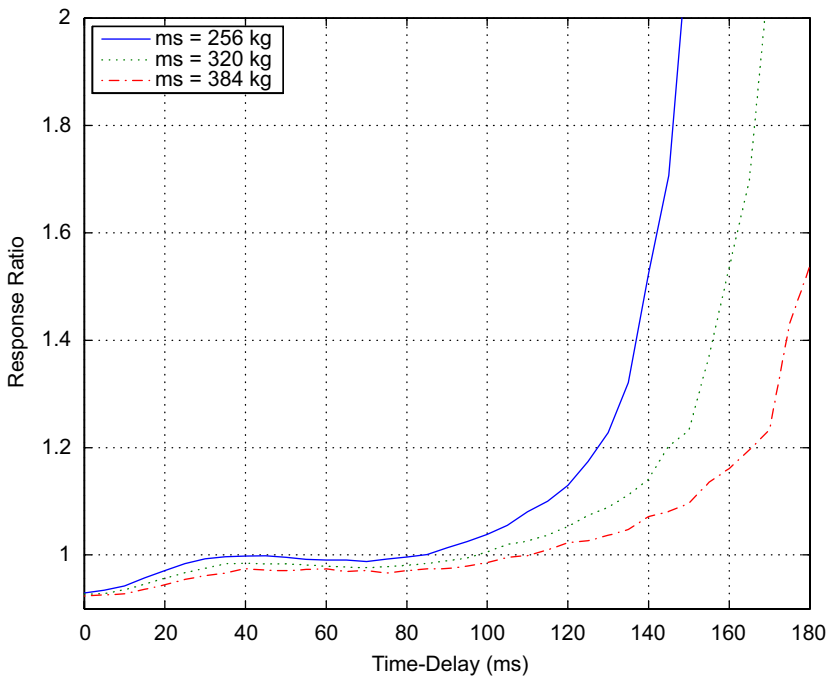

Fig. 5. rms ratio between active suspension and passive suspension for sprung mass acceleration versus actuator time delay (full state feedback control case).

where $\Omega_0 = 1/2\pi$ is a reference spatial frequency, Ω is a spatial frequency. The value $S_g(\Omega_0)$ provides a measure for the roughness of the road. n_1 and n_2 are road roughness constants. The ISO has proposed road roughness classification using the PSD values as listed in Table 3.

In particular, for vehicle models, samples of the random road profiles can be generated using the spectral representation method [31]. If the vehicle is assumed to travel with a constant horizontal speed v_0 over a given road, the road irregularities can be simulated by the following series

$$z_{rf}(t) = \sum_{n=1}^{N_f} s_n \sin(n\omega_0 t + \varphi_n), \tag{45}$$

where $s_n = \sqrt{2S_g(n\,\Delta\Omega)\Delta\Omega}$, $\Delta\Omega = 2\pi/L$, L is the length of the road segment considered, $\omega_0 = (2\pi/L)v_0$, φ_n is treated as random variables following a uniform distribution in the interval $[0, 2\pi)$, N_f limits the frequency range to be considered.

In this paper, $n_1 = 2$, $n_2 = 1.5$, $L = 100$, $N_f = 200$ are used to generate the random road profiles. Taking into account the random nature of the excitation applied, the root mean square (rms) for the random responses of sprung mass acceleration, suspension deflection, and tyre deflection will be evaluated. For each case, 50 random tests are used to compute the expected rms values.

To show the results clearly, we only plot the rms ratio between the active suspension and the passive suspension for sprung mass acceleration in Fig. 5, where the sprung mass is given as the nominal value and the two-vertex cases for one type of road roughness (C, average) and one selected vehicle forward velocity 72 km/h. It can be seen from Fig. 5 that in spite of the variation of sprung mass, the sprung mass acceleration of active suspension is always less than the passive suspension (the response ratio is less than 1) within time delay $\tau \leqslant 50$ ms. It shows that the designed active suspension could achieve good ride comfort performance within the indicated delay bound in spite of the variation of sprung mass within allowable range.

Fig. 6 shows the PSD of sprung mass acceleration for the active suspension and the passive suspension. To show the curves clearly, only those cases that the sprung mass is given as the nominal value and the two-vertex cases are plotted, respectively. The road roughness (C, average), the vehicle forward velocity 72 km/h, and the

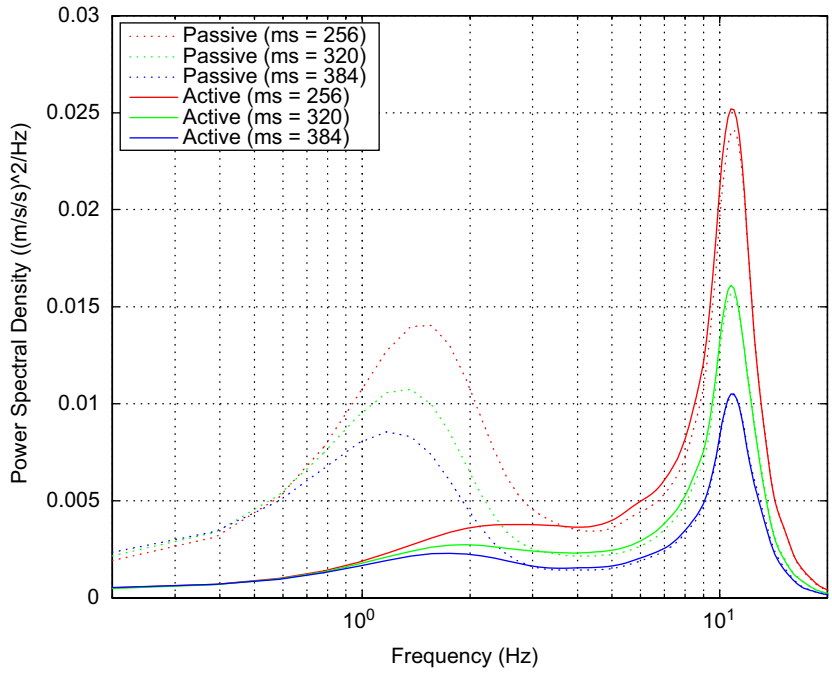

Fig. 6. PSD of sprung mass acceleration under a random road profile (C, average) at vehicle speed 72 km/h with time delay $\tau = 10$ ms (full state feedback case).

actuator time delay $\tau = 10$ ms are used. It is clearly seen from Fig. 6 that the active suspension achieves a significant improvement on ride comfort regardless of the sprung mass variation and the actuator time delay.

4.2. Static output feedback control case

In practice, not all the state variables are measurements available for control. Therefore, a static output feedback parameter-dependent controller, which uses easily available measurements, needs to be designed. Since the suspension deflection ($x_1(t)$) can be measured using suitable displacement transducer, and the sprung mass acceleration can be straightforwardly measured using accelerometer, and in principle, the sprung mass velocity ($x_3(t)$) can be obtained by integrating the sprung mass acceleration signal accordingly, we prefer to using suspension deflection and sprung mass velocity as feedback signals to design such a static output feedback controller. Using the same algorithm as presented in the last section with an appropriate C matrix given by

$$C = \begin{bmatrix} 1 & 0 & 0 & 0 \\ 0 & 0 & 1 & 0 \end{bmatrix}$$

the static output feedback parameter-dependent controller gains are obtained as

$$K_1 = 10^3 \times [-4.9709 \quad -2.8662], \; K_2 = 10^3 \times [-4.9356 \quad -2.3330].$$

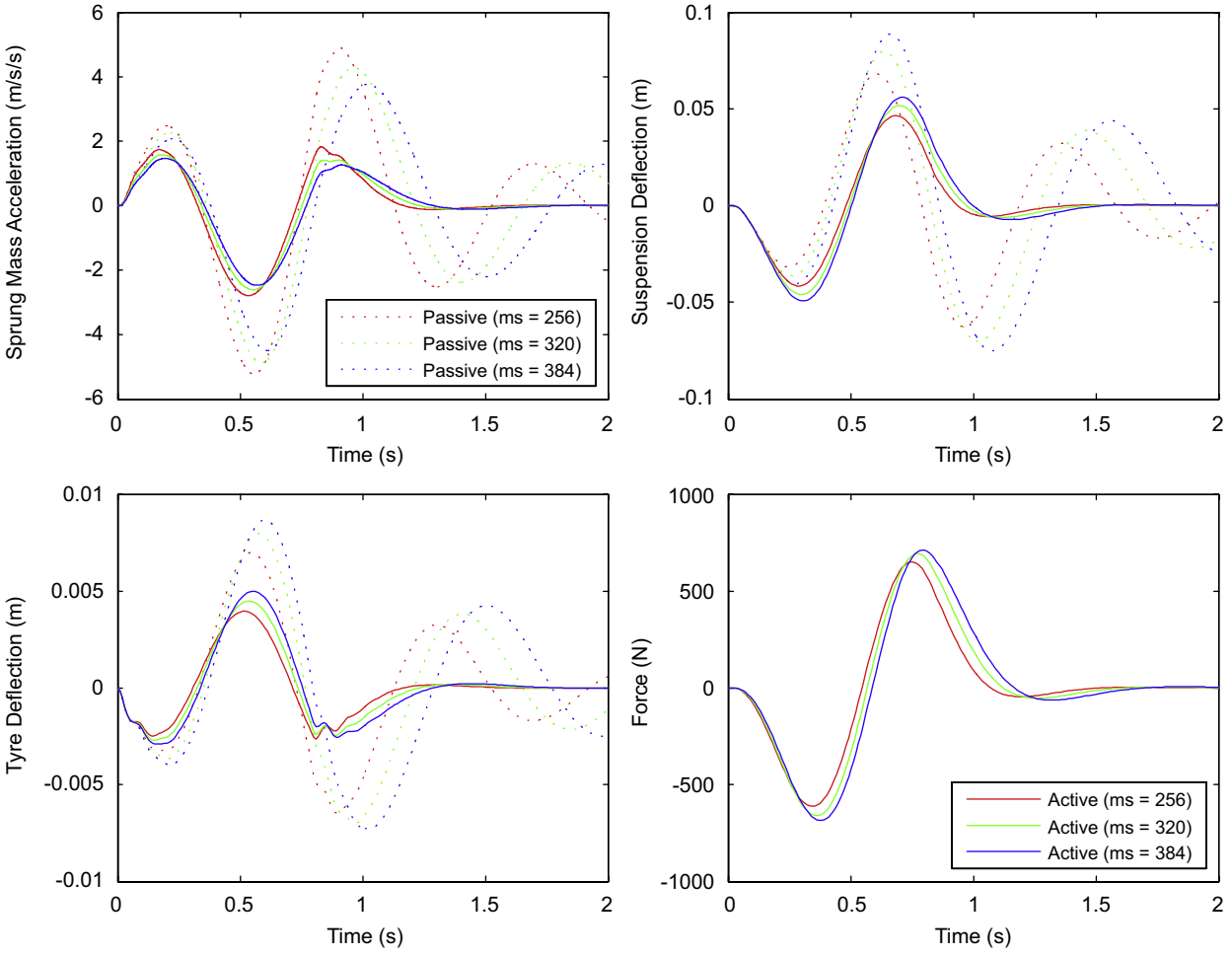

Fig. 7. Bump response for static output feedback control case with time delay $\tau = 0$ ms. The legends shown in upper-left and lower-right plots are used for all plots in this figure.

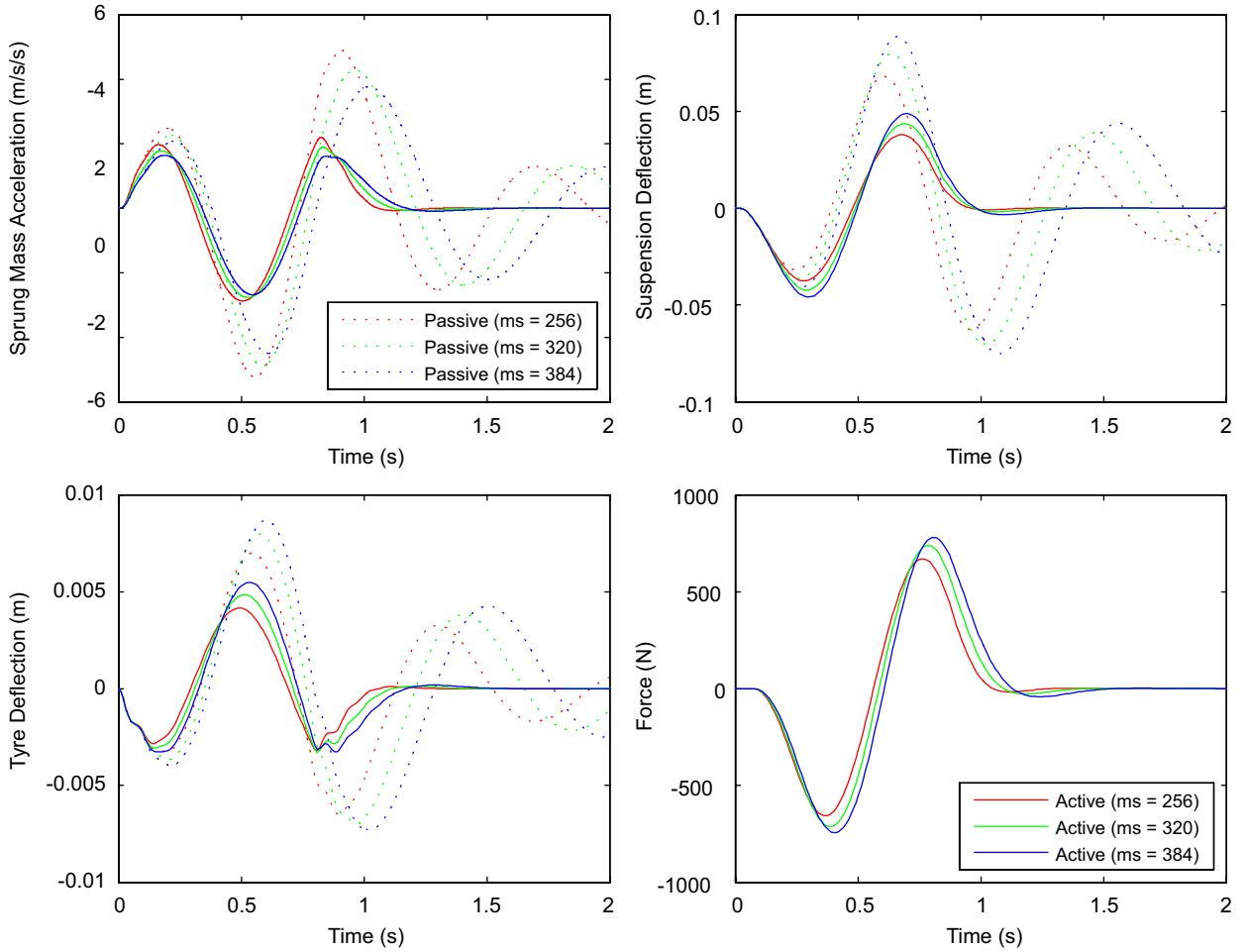

Fig. 8. Bump response for static output feedback control case with time delay $\tau = 50$ ms. The legends shown in upper-left and lower-right plots are used for all plots in this figure.

Table 4
Comparison of maximum peak value for bump response (static output feedback control case)

	Passive			Active					
				$\tau = 0$ ms			$\tau = 50$ ms		
m_s (kg)	256	320	384	256	320	384	256	320	384
$\dot{x}_{3\max}$ (m/s^2)	5.2255	4.8756	4.4959	2.7887	2.6073	2.4723	2.8675	2.7631	2.6776
$x_{1\max}$ (m)	0.0681	0.0799	0.0889	0.0465	0.0518	0.0561	0.0380	0.0438	0.0489
$x_{2\max}$ (m)	0.0070	0.0080	0.0087	0.0040	0.0045	0.0050	0.0042	0.0048	0.0055
$u_{\max}$ (N)	–	–	–	650.87	694.34	712.87	669.88	738.29	780.75

The performance evaluation of the designed controller is done similarly as that for full state feedback control case. The bump responses are plotted in Figs. 7 and 8, for time delay as 0 and 50 ms, respectively. The maximum peak response values are given in Table 4. For designed active suspension, it can be seen that the maximum peak values are similar for both $\tau = 0$ and 50 ms cases.

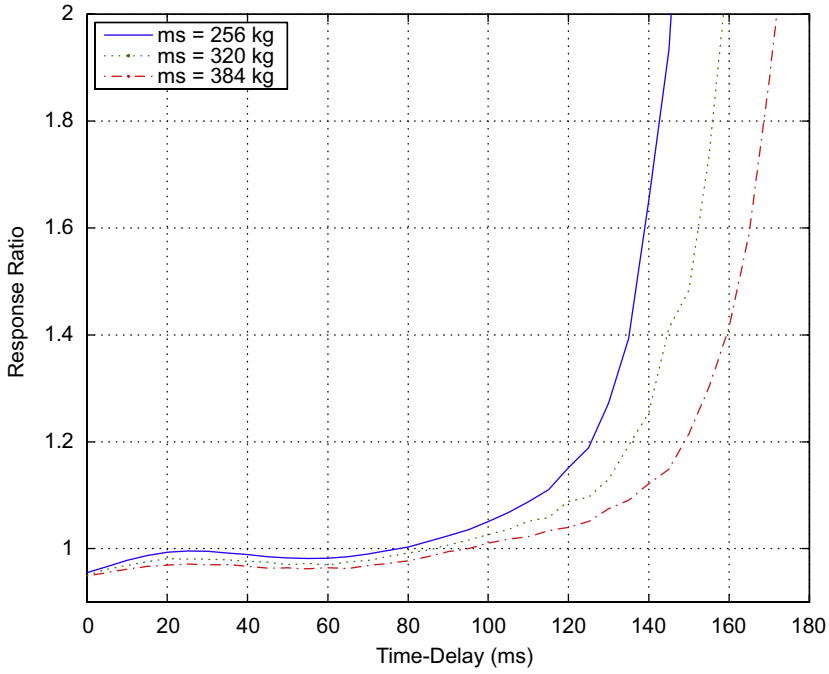

Fig. 9. rms ratio between active suspension and passive suspension for sprung mass acceleration versus actuator time delay (static output feedback control case).

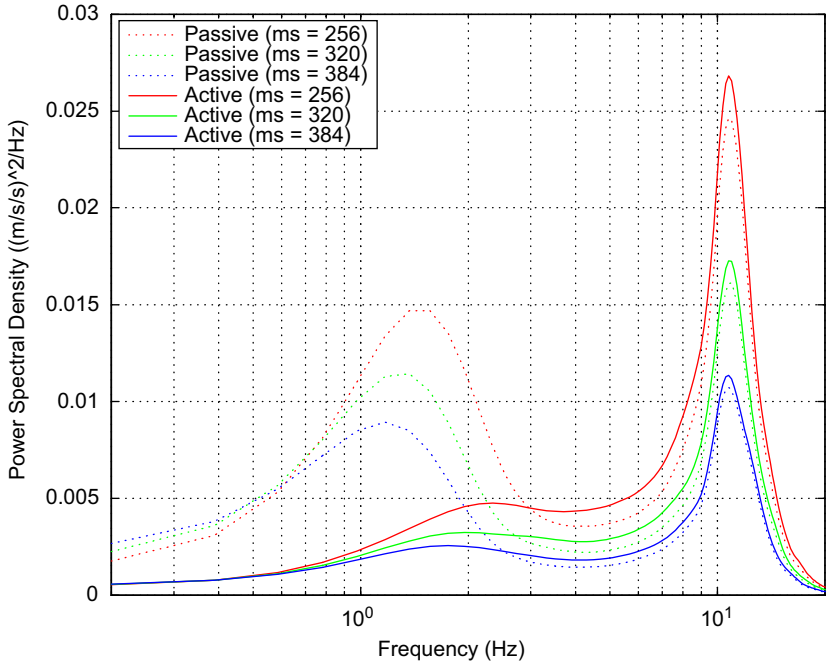

Fig. 10. PSD of sprung mass acceleration under a random road profile (C, average) at vehicle speed 72 km/h with time delay $\tau = 10$ ms (static output feedback case).

The RMS ratio between the active suspension and the passive suspension for sprung mass acceleration for one type of road roughness (C, average) and one selected vehicle forward velocity 72 km/h is plotted in Fig. 9, where the sprung mass is given as the nominal value and the two-vertex cases, respectively. Similarly, it can be

seen that the sprung mass acceleration of active suspension is less than the passive suspension within time delay $\tau \leqslant 50$ ms.

Similarly, the PSD of sprung mass acceleration for the active suspension and the passive suspension is shown in Fig. 10, where the cases that the sprung mass is given as the nominal value and the two-vertex cases are plotted for clarity, and the road roughness (C, average), the vehicle forward velocity 72 km/h, and the actuator time delay $\tau = 10$ ms are used. It can be seen that a significant improvement on ride comfort is achieved by the active suspension regardless of the sprung mass variation and the actuator time delay.

The simulation results verify that, using the same algorithm, the designed static output feedback controller can realise the similar performance to that of full state feedback controller when the sprung mass has uncertainty and the actuator time delay is present.

5. Conclusions

This paper presents a parameter-dependent controller design approach for vehicle suspension with considerations on changes in vehicle inertial parameters and existence of actuator time delays. In order to reduce the conservativeness of the presented controller design conditions, parameter-dependent Lyapunov functional is used. Based on the identification technique recently developed for accurate estimations of inertial parameters, the presented parameter-dependent controller could be implemented in practice. Furthermore, the controller that only uses the easily available measurements, such as sprung mass velocity and suspension deflection, is designed in the same way. The designed controllers are applied to a quarter-car suspension model with large change in sprung mass and large time delay in input. Numerical simulations have validated that the vehicle suspension performance is improved with the designed controller in spite of the sprung mass variation and actuator time delay.

Acknowledgements

The supports of this work by the Australian Research Council's Discovery Projects funding scheme (Project no. DP0560077) and RGC Grant HKU 7031/06P are gratefully acknowledged.

References

[1] D. Hrovat, Survey of advanced suspension developments and related optimal control applications, *Automatica* 33 (10) (1997) 1781–1817.

[2] R.A. Williams, Automotive active suspensions, *Proceedings of the Institute of Mechanical Engineers Part D: Journal of Automobile Engineering* 211 (1997) 415–444.

[3] J. Wang, D.A. Wilson, Mixed $GL_2/H_2/GH_2$ control with pole placement and its application to vehicle suspension systems, *International Journal of Control* 74 (13) (2001) 1353–1369.

[4] J. Lu, M. DePoyster, Multiobjective optimal suspension control to achieve integrated ride and handling performance, *IEEE Transactions on Control Systems Technology* 10 (6) (2002) 807–821.

[5] H. Chen, K. Guo, Constrained H_∞ control of active suspensions: an LMI approach, *IEEE Transactions on Control Systems Technology* 13 (3) (2005) 412–421.

[6] H. Chen, Z.Y. Liu, P.Y. Sun, Application of constrained H_∞ control to active suspension system on half-car models, *Journal of Dynamic Systems, Measurement, and Control* 127 (2005) 345–354.

[7] H. Gao, J. Lam, C. Wang, Multi-objective control of vehicle active suspension systems via load-dependent controllers, *Journal of Sound and Vibration* 290 (2006) 654–675.

[8] F. Momiyama, K. Kitazawa, K. Miyazaki, H. Soma, T. Takahashi, Gravity center height estimation for the rollover compensation system of commercial vehicles, *JSAE Review* 20 (1999) 493–497.

[9] G. Venture, P. Bodson, M. Gautier, W. Khalil, Identification of the dynamic parameters of a car, *SAE 2003 World Congress*, no. 2003-01-1283, Detroit, USA, 2003.

[10] A. Vahidi, A. Stefanopoulou, H. Peng, Recursive least squares with forgetting for online estimation of vehicle mass and road grade: theory and experiments, *Vehicle System Dynamics* 43 (1) (2005) 31–55.

[11] M. Rozyn, N. Zhang, G. Dissanayake, Identification of inertial parameters of an on-road vehicle, *SAE International Conference on Noise and Vibration*, no. 2007-01-2220, Illinois, USA, 2007.

[12] A. Alleyne, R. Liu, On the limitations of force tracking control for hydraulic servosystems, *Journal of Dynamic Systems, Measurement, and Control* 121 (2) (1999) 184–190.

[13] A. Alleyne, J.K. Hedrick, Nonlinear adaptive control of active suspensions, *IEEE Transactions on Control Systems Technology* 3 (1) (1995) 94–101.
[14] Z.H. Wang, H.Y. Hu, Stability switches of time-delayed dynamic systems with unknown parameters, *Journal of Sound and Vibration* 233 (2) (2000) 215–233.
[15] H. Du, N. Zhang, H_∞ control of active vehicle suspensions with actuator time delay, *Journal of Sound and Vibration* 301 (1) (2007) 236–252.
[16] A. Alleyne, P.D. Neuhaus, J.K. Hedrick, Application of nonlinear control theory to electronically controlled suspensions, *Vehicle System Dynamics* 22 (5) (1993) 309–320.
[17] A.G. Thompson, B.R. Davis, Force control in electrohydraulic active suspensions revisited, *Vehicle System Dynamics* 35 (3) (2001) 217–222.
[18] S. Chantranuwathana, H. Peng, Adaptive robust force control for vehicle active suspensions, *International Journal of Adaptive Control and Signal Processing* 18 (2) (2004) 83–102.
[19] P.C. Chen, A.C. Huang, Adaptive sliding control of active suspension systems with uncertain hydraulic actuator dynamics, *Vehicle System Dynamics* 44 (5) (2006) 357–368.
[20] N. Jalili, E. Esmailzadeh, Optimum active vehicle suspensions with actuator time delay, *Journal of Dynamic Systems, Measurement, and Control* 123 (2001) 54–61.
[21] H. Du, J. Lam, K.Y. Sze, Non-fragile output feedback H_∞ vehicle suspension control using genetic algorithm, *Engineering Applications of Artificial Intelligence* 16 (8) (2003) 667–680.
[22] Y. He, M. Wu, J.H. She, G.P. Liu, Parameter-dependent Lyapunov functional for stability of time-delay systems with polytopic-type uncertainties, *IEEE Transactions on Automatic Control* 49 (5) (2004) 828–832.
[23] H. Gao, P. Shi, J. Wang, Parameter-dependent robust stability of uncertain time-delay systems, *Journal of Computational and Applied Mathematics* 206 (1) (2007) 366–373.
[24] L. Zhang, P. Shi, E.-K. Boukas, C. Wang, H_∞ control of switched linear discrete-time systems with polytopic uncertainties, *Optimal Control Applications and Methods* 27 (5) (2006) 273–291.
[25] C. Lin, Q.-G. Wang, T.H. Lee, A less conservative robust stability test for linear uncertain time-delay systems, *IEEE Transactions on Automatic Control* 51 (1) (2006) 87–91.
[26] R.M. Palhares, P.L.D. Peres, Robust filtering with guaranteed energy-to-peak performance—an LMI approach, *Automatica* 36 (2000) 851–858.
[27] T. Gordon, C. Marsh, M. Milsted, A comparison of adaptive LQG and nonlinear controllers for vehicle suspension systems, *Vehicle System Dynamics* 20 (1991) 321–340.
[28] H. Gao, T. Chen, J. Lam, A new delay system approach to network-based control, *Automatica* 44 (2008) 39–52.
[29] H. Gao, C. Wang, Comments and further results on a descriptor system approach to H_∞ control of linear time-delay systems, *IEEE Transactions on Automatic Control* 48 (3) (2003) 520–525.
[30] H. Du, N. Zhang, J. Lam, Computation of robust H_∞ controllers for time-delay systems using genetic algorithms, *Control and Intelligent Systems* 35 (4) (2007) 395–400.
[31] G. Verros, S. Natsiavas, C. Papadimitriou, Design optimization of quarter-car models with passive and semi-active suspensions under random road excitation, *Journal of Vibration and Control* 11 (2005) 581–606.